White Blood Cells Recognition System Based on Deep Residual Network

Sultan Almotairi[1,*] **and A.I. Shahin**[2]
[1] Department of Natural and Applied Sciences, Community College,
Majmaah University, Al- Majmaah 11952, Saudi Arabia
[2] Department of Biomedical Engineering, HTI, Egypt.
[*] Corresponding author: almotairi@mu.edu.sa

Summary
Recently, several automated blood analysis systems (ABAS) have been developed based on image processing and artificial intelligence techniques. White blood cells differential counting and recognition aim to diagnose several human diseases. In the present study, a recognition system of five healthy white blood cells has been demonstrated. Deep learning methodologies have gained significant importance among artificial intelligence techniques for several ABAS. In this paper, we propose a white blood cells recognition system based on the residual deep network. We increase the performance of the previous recognition system based on three approaches which are residual blocks, dropout layer, and batch normalization layers. To save the computational power and cost time, we optimize the location of residual block inside the plain CNN network. A significant improvement has been achieved by the proposed system. The achieved results contribute to increasing either the traditional recognition system or deep learning system performance. During our experiments, we employ two white blood cells datasets which contain 2426 cropped images for different main five white blood cells (WBCs) classes. The proposed network achieves 96.8% accuracy and 96.4% sensitivity. Moreover, we re-employ the proposed system as a pre-trained network to recognize limited size WBCs dataset. Based on transfer learning, the proposed system achieved 95.83% for recognition limited size dataset. We visualize deep features to prove the power of our propped deep network. The experimental results show promising results for our proposed approach.

Key words:
Blood Smear Image, Deep learning, CNN, Residual Networks, WBCs Identification.

1. Introduction

Blood smear microscopic images consist of white blood cells (WBCs), red blood cells (RBCs), and platelets [1]. With the advantage of computer vision modern systems, each blood component can be analyzed using computer vision systems. Each blood component disorder refers to a body disorder, so several diseases can be diagnosed through a blood smear microscopy image. Health WBCs play an important role in controlling the body immune system. Since it is important to recognize its several types which are divided into five types as shown in Fig.1.

Each WBC has its own nucleus and cytoplasm structure. All WBCs types differentiate in size, color, and texture. On the other hand, RBCs have no nuclei [2].

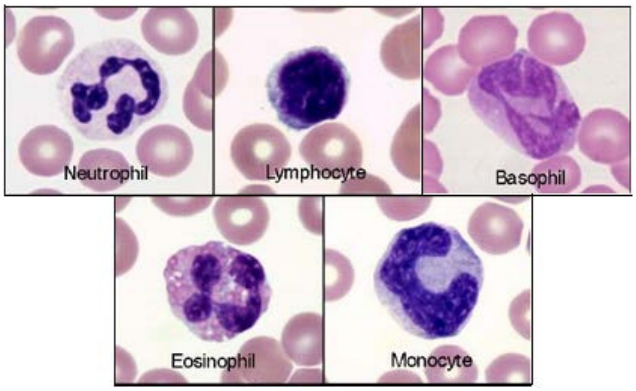

Fig. 1 Five main WBCs types (neutrophil, lymphocyte, basophil, eosinophil, and monocyte).

Traditional ABAS consists of consequences steps such as enhancement, segmentation, feature extraction, feature selection (FS), and classification [3]. A lot of research articles had been introduced through the last decade which employed the traditional ABAS techniques [4-14]. A lot of drawbacks was found inside traditional one such as the sensitivity to lighting conditions, cell staining contrast, cell morphological orientation. Besides that, the handcrafted features process consumed a lot of time and did not achieve the highest performance [3]. Recently, a lot of research articles employ deep learning techniques to increase the performance of traditional ABAS [3, 15- 21].
Deep learning is a recent artificial intelligence theory which exponentially grows up in the last decade. LeCun [22] introduced the convolutional neural network (CNN) which aims to automatically produce learned features by applying several convolutions of the input image, then the process is repeated into network depth. Near to the network output, the learned feature map should have more useful information.
There are several architectures were introduced State of art CNN (LeNet-5) consists of several layers such as image input layer, convolutional layer, activation function,

Manuscript received October 5, 2019
Manuscript revised October 20, 2019

pooling layer, fully-connected layer, and classification layer [22]. Then, AlexNet [23], VGGNet architecture with its both models VGG16 and VGG19 had been introduced as more-depth networks with the same sate of art layers [24]. Google Inception architecture had been also introduced with more layers connectivity and more depth network [25]. ResNet architecture with its models ResNet 18, 50,101 based on the residual network had been proven as an excellent tool [26]. Moreover, it had been proven that the conversion of plain networks to residual network increase the recognition system performance such as VGGNet [27]. Deep learning increased the performance of several automated medical diagnosis systems [28-38].

In contrast to the general images' dataset size, the dataset size of medical applications severe from its low size. For this challenge, there are several strategies used to employ deep learning techniques with medical applications such as DeCA approach [39] and transfer learning approach [40-41]. However, the training of network from scratch still is one of the best strategies that achieved the highest performance [41]. On the other hand, the availability of modern graphics processing unit (GPUs) technologies helps to run CNN computation faster than traditional central processing unit (CPUs). Such technologies help to produce low depth optimized architectures to solve medical recognition task.

The rest of the paper is organized as the following. In the next section, the literature review for WBCs recognition systems based on deep learning is presented. Then, in section 3, the proposed recognition system is described. In section 4, the results and discussions section are introduced. Finally, the conclusion is presented.

2. Literature Review

In this section, Firstly, we demonstrate a survey for the traditional WBCs recognition systems and especially the one that used the same WBCs dataset in our work. Secondly, the first deep learning version of WBCsNet network that had been applied to the same WBCs dataset in our work. Thirdly, recent works that employed a deep learning approach to solve WBCs recognition task, Finally, we introduce the need and our main contribution in this work.

In the last decade, several approaches were applied to move forward the traditional WBCs recognition systems [8-13]. In the most recent work [9], traditional WBCs recognition utilized several image processing enhancement algorithms to overcome staining variability issue [42]. However, we cannot generalize enhancement procedures with different stains. Most researches were performed in two levels to extract WBC nucleus and recognize the cytoplasm region [8]. However, a lot of morphological processing and filtering were applied to solve segmentation errors. Several articles were established based on two-step of classification. This also consumed a lot of processing time. Moreover, such systems cannot be generalized or utilized with other data sources.

In [9], a traditional WBCs recognition system based on isolation and two-step classification. The authors employed a pre-processing color transformation to overcome unstable lighting conditions. Thresholding had been applied to extract cell structure. Finally, the system classified the cell is segmented or not, then classify them into main 5 healthy WBCs. The system consumed a lot of time in the pre-processing stage and classification. Moreover, the system achieved only 93.9% accuracy.

In [41], the authors presented a novel plain CNN called WBCsNet. WBCsNet consists of 3 convolutional layers, two pooling layers, two fully connected layers, and a classification layer. The image input layer size had been investigated to achieve the best performance. Moreover, WBCsNet had been examined for transfer learning task and classify limited WBCs dataset size. The system accuracy reached to 96.1%.

Recently, several kinds of articles proposed a deep learning approach to solve our problem [15-16, 20-21]. Most works in the literature were based on low depth plain CNN network [15]. In [20], the authors classified 1295 WBCs for only 3 non-healthy cells. The network consisted of 5 layers and achieved only 92.8%. In [43], the authors tried to classify limited WBCs dataset size with 11 layers. They trained their network from scratch, however, the low size of dataset affected on the achieved performance with accuracy 80%. In [44], the authors introduced a deep learning model based on transfer learning. They applied a fine-tuning to LeNet architecture. However, the cells were processed in the gray-scale level. This decreased system performance and achieved 84.7% accuracy. In [4], a WBCs recognition system had been presented based on deep features fusion. The authors extended no. of layers to 19 layers. They had also extended the no. of classes to 5 healthy WBCs and 6 RBCs types. They trained their algorithm on 64000 cells from different datasets. They achieved 95.1% accuracy. In [18], the authors built a recognition model based on transfer learning approaches and employ VGGNet -16 which is also a plain network. The achieved accuracy was 93.15%, however, the fine-tuning of VGGNet-16 required long training time. Since there is a real need to employ new deep layers and residual network to increase the previous system performance with minimum computation power.

In this paper, our contributions are as follows. We propose a novel WBCsNet-2 for white blood cells recognition task. The proposed system process two different WBCs datasets. The first WBCs dataset is the same dataset used before to train the old plain WBCsNet. We compare its performance with the new proposed recognition system WBCsNet. The second WBCs dataset is used to investigate the WBCsNet-

2 for transfer learning theory. We achieve a significant improvement in the performance of old plain WBCsNet network based on residual blocks. We optimize the location of residual block inside the network to save the computational power and save the network depth. All deep features are visualized for a sample cell to illustrate how the network is robust.

3. Proposed Method

For several reasons, deep learning still represents a powerful classification tool for many medical diagnosis applications. Since there are many techniques have been introduced to increase the plain CNN performance. There is a real need to develop old WBCsNet that have been employed to classify 5 health WBCs with more accuracy. In the next section, we introduce several deep layers functions which are employed to extract the deep features and recognize our classification task.

The convolutional layer consists of a set of convolutional filters. These filters are associated with a spatial area of the image known as a receptive field. The image is divided into small blocks and convolving them with a specific set of filters which represent learned weights. The convolution operation is explained in Eq (1):

$$F_I^K = I_{x,y} * K_I^k \quad (1)$$

where $I_{x,y}$ represent input image (x, y), K_I^k represents I^{th} convolutional kernel of k^{th} layer.

The averaging pooling layer is used to perform down sampling the input image and decrease computational complexity as defined in Eq (2)

$$Z_I = f_p(F_{x,y}^I) \quad (2)$$

where Z_I represents I^{th} output feature map, $F_{x,y}^I$ represents I^{th} input feature map, and f_p represents pooling operation type.

The Relu activation function has been proven a fast and robust activation function for CNN architectures [46].

$$T_I^k = f_A(F_I^k) \quad (3)$$

F_I^k represent the output of convolution layer operation, and f_A represents the activation ReLU function [47].

Batch normalization (BN) increases CNN stability, by normalizing the output of a previous activation layer and subtracting the batch mean and dividing by the batch standard deviation. This also accelerates deep network training by reducing internal covariate shift. Batch normalization for transformed feature map T_I^k is defined in Eq (4).

$$N_I^k = \frac{T_I^k}{\sigma^2 + \sum_i T_i^k} \quad (4)$$

N_I^k represents the feature map after the normalization process, T_I^k represents input feature map, and σ represents variation through the feature map.

Dropout layer presents the regularization concept within a network. This happens by stochastically "dropping out" some neurons during training to avoid the co-adaptation of feature detectors. The dropout concept helps to prevent over-fitting.

Fully connected (FC) layer is the last layer before the classification layer which is a global operation. In the classification problems, CNN has two FC layers. The first prepares the feature map data from the CNN network and arranges it into a feature matrix form. The second one is adjusted to the number of classification problem classes.

Residual CNN was proposed in the ResNet network architectures by He et al. [48]. The single residual network can be achieved as shown in Fig.2. Only the disadvantage of deep ResNet architectures is the highest required computational power, as it was 8-20 times deeper than plain AlexNet. In the previous studies [49], residual block increases the performance of plain CNN network about 28%.

On the other hand, the residual networks improve several plain networks performance like VGGNet16 and 19 [27]. However, the increasing of network depth, increase the computational complexity and training cost time. For these reasons, we propose a novel WBCsNet-2 based on a residual concept.

Softmax classifier [50] is used to classify the 32- sign language class. Softmax classifier determines the normalized probability score for each class. The Softmax function is defined in eq (5).

$$f_i(z) = \frac{e^{z_j}}{\sum_k e^{z_k}} \quad (5)$$

where the function takes a vector of arbitrary real-valued scores (in z) and compresses it to a vector of values between zero and one that sums to one. The cross-entropy loss is used to obtain class scores f which is formulated in Eq. (6).

$$L_i = f_{y_i} + log \sum_j e^{f_j} \quad (6)$$

where the f_j refers to the j_{th} element of the vector of class scores f [50].

3.1 WBCsNet-2 Architecture

As shown in Fig.3, WBCsNet and its modified version WBCsNet-2 are shown. WBCsNet consists of plain CNN layers with no dropout or even batch normalization layer. In WBCsNet-2, we achieve a residual concept by modifying the first convolutional layer inside old WBCsNet to a residual network as shown in Fig.3. The advantage of first convolutional layer modification is the low number of filters founded in first layers, despite the

highest number of filters excited in late layers. Then, to increase the performance of the proposed system, we add batch normalization layer for each convolutional unit. Finally, the dropout layer has been added to overcome overfitting.

In our proposed WBCsNet-2, the first residual block consists of 3 convolutional layers. Each Conv1 layer dimension is chosen to be 5×5×64 with mask dimension is 5×5. Conv1 contains 64 filters which are applied to do the sub-sampling. Conv1 stride is chosen to be 1 with zero padding. Each Conv1 layer is followed by BC layer and ReLU activation function. Then, the additional layer is added after the last Conv1 layer and followed by ReLU activation function. Finally, a maximum pooling layer (Pool1) are applied with filter dimension 2×2 and zero padding.

Plain layer 1 consists of a single convolutional unit Conv2 layer size is chosen to be 5×5×256 with filter dimension is 5×5. Conv2 contains 256 filters which are chosen to perform the sub-sampling. Conv2 stride is chosen to be 1 with zero padding. Conv2 layer is followed by BC layer and ReLU activation function. Finally, a maximum pooling layer (Pool2) are applied with filter dimension 2×2 and zero padding.

Plain layer 2 consists of a single convolutional unit Conv4 layer dimension is chosen to be 3×3×512 with filter dimension is 3×3, where 512 filters are applied to perform the sub-sampling. Stride is chosen to be 1 with zero padding. Conv3 layer is followed by BC layer and ReLU activation function.

In WBCsNet-2, the first fully-connected layer (FC1) is set to 512 to fit with extracted deep features. FC1 layer is followed dropout layer. The final fully-connected layer (FC2) contains the 5-classes of healthy WBCs. Our final features matrix dimension should be 5×512.

One of the advantages of the proposed network its low feature pool dimension compared to the other pre-trained networks. This helps us to employ the cross-validation technique with 10-folds to evaluate the proposed system as followed in [41]. This leads to an independent dataset without over-fitting and generates a model which can accurately be a predictive model and has more reality in practice.

4. Experimental Results

In this paper, two public datasets called; Dataset1 and Dataset2. Both datasets contain five healthy WBCs classes which were manually cropped. Dataset1 [9] was captured at 20×magnification and contains 320 images. Each cropped WBC resolution is 70×70 pixels and stored in TIF format. Dataset2 was captured with magnification lens 100X [7] and collected from 100 microscopic image. Each microscopic image resolution is 720×576 pixels and stored in BMP format, and each WBC resolution is 150×150.

During our experiments, our algorithms are performed using the MATLAB 2019 a. The system platform containing Quad-Core 2.9 GHz Intel i5 with 16GB RAM. To speed up the training process, we employ NVIDIA TITAN-Xp GPU with 12 GB RAM.

The performance of previous WBCs recognition systems was evaluated using accuracy, specificity, sensitivity … etc. As followed in [41], our comparative results for our approach is evaluated using similar metrics. We utilize the confusion matrix and its results such as False negative (FN), FP False positive (FP), and True negative (TN). In [41], the average of many evaluation parameters is computed to evaluate the approach performances is calculated as follows:

$$Accuracy = \frac{TP+TN+FP+FN}{TP+FN} \quad (7)$$

$$Sensitivity = \frac{TP}{TP+FN} \quad (8)$$

$$Specifity = \frac{TN}{TN+FP} \quad (9)$$

We propose the experimental results into three sub-sections: training results, testing results, and transfer learning results. We investigate the performance of the pre-trained network through transfer learning. Our comparison is based on the previous evaluation parameters (Eq. (7) to Eq. (9)), training cost time, and confusion matrix.

4.1 Training Results

We employ SGD optimizer for the training process and select 40 epochs to ensure that the training phase will be converged as followed in [41] with min-batch size 32. The initial learning rate setup is 0.001. We evaluate the performance of each pre-trained network during the training process through training accuracy versus iteration number, loss function versus iteration number, and training cost time. In Fig. 4, the learning accuracy curves starts from 40% accuracy and finish the training with accuracy 100%. On the other hand, In Fig. 5, the learning loss curves starts from 1.65 and finish the training process at zero loss.

4.2 Testing Results

In this section, all experiments were based on Dataset1 which contains 2172 cells. We utilize the large dataset to train the proposed system from scratch.

In this experiment, we investigate the proposed system accuracy vs. previous approaches as shown in Fig.6. The proposed WBCsNet-2 achieved 96.8% accuracy more than WBCsNet which achieved 96.1%. A significant

improvement 0.7% achieved by adding a residual block, batch normalization, and dropout layers. On the other hand, both recognition systems based on deep learning achieved more accuracy than traditional one. Transfer learning approach for LeNet and AlexNet achieve the lowest accuracy score.

In Fig.7, the other evaluation parameters are shown. We compare between WBCsNet and WBCsNet-2 based on sensitivity and specificity metrics. The proposed WBCsNet-2 enhance the system sensitivity score to 92.63%. However, a slight increase in the specificity metric has been noticed with 0.02%.

The confusion matrix of WBCsNet-2 recognition system is shown in Table.1. It is noticed that the true positive value of Neutrophil cell recognition increased to 1401. The old WBCsNet achieved 1382 true positive value for Neutrophil cell. Moreover, Basophil cell with its low number has no false negative value. The misclassification between Eosinophil cell and Neutrophil cell has been noticed. This misclassification can be explained by high similarity in their cell structure. On the other hand, a misclassification has been also noticed between Lymphocyte and Monocyte cell. This misclassification can be explained by their nucleus texture similarity.

4.3 Transfer learning using WBCsNet-2

In this section, all experiments were based on Dataset2 which contains 254 cells. We utilize the low size dataset to perform transfer learning process. Employing the trained network as a pre-trained network was addressed in [40]. The proposed WBCsNet-2 achieved accuracy based on transfer learning 95.8%. A significant improvement reaches to 2.4% has been achieved using our proposed system as shown in Fig.8.

CNN features visualization assist in the power of the training of deep learning systems. It also reflects the robust of the proposed model. Each convolutional unit contains no. of learned filters. The most bight and dark pixels represent the highest activation response. On the other hand, the gray pixels reflect low response. In this experiment shown in Fig.9, we select the Neutrophil cell according to its high percentage inside WBCs Dataset. We address the cell activation through the first convolution unit (Conv1) which consists of three convolutional layers, the second convolutional unit which consists of a single convolutional layer (Conv2), and, the third convolutional unit which consists of a single convolutional layer (Conv3). Cov1 consists of 64 filters, Conv2 consists of 256 filters, and Conv3 consists of 512 filters. It is noticed that in deeper convolutional units, the features of the learned filter are more complicated as it should contain obvious features about the network which had been learned.

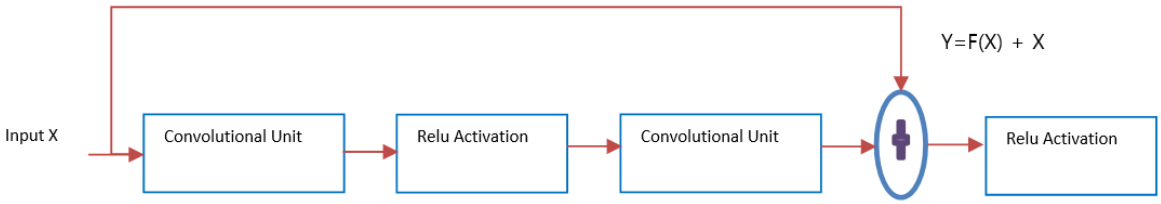

Fig. 2 Single residual network architecture.

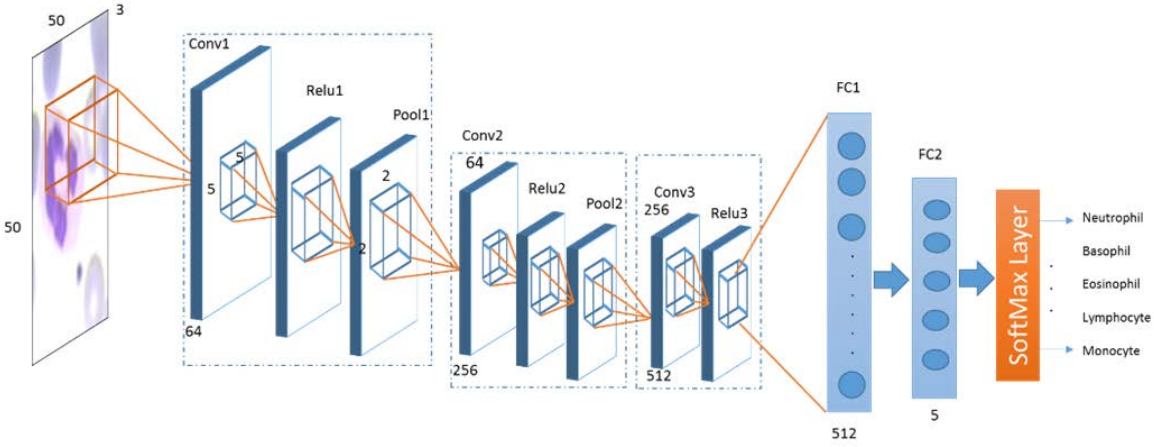

(a)

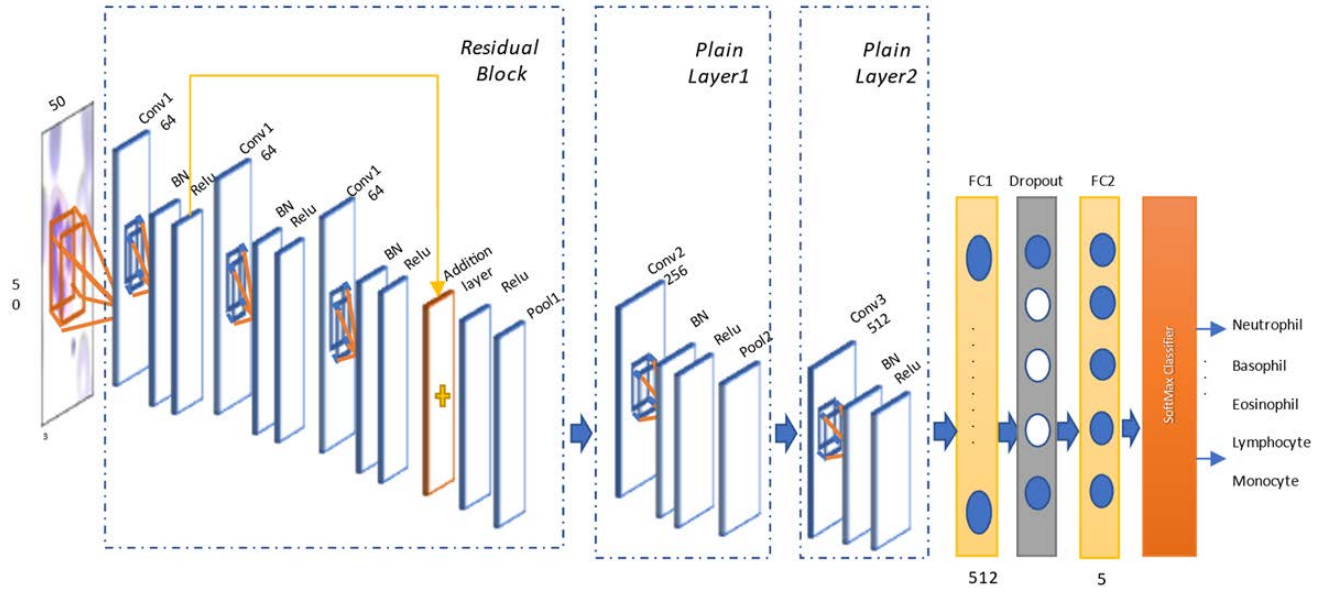

(b)

Fig. 3 (a) WBCsNet architecture, (b) The proposed WBCsNet-2 architecture.

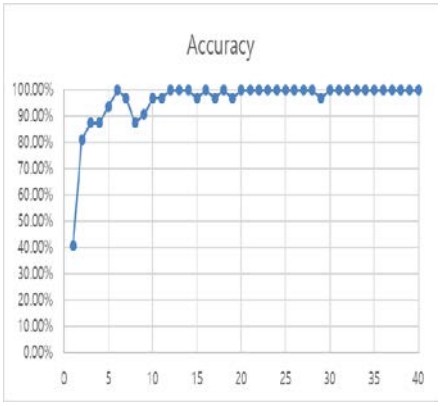

Fig. 4 The proposed WBCsNet-2 architecture training accuracy performance.

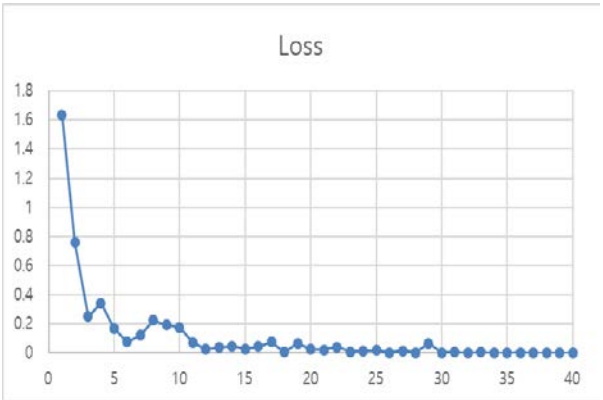

Fig. 5 The proposed WBCsNet-2 architecture training loss performance.

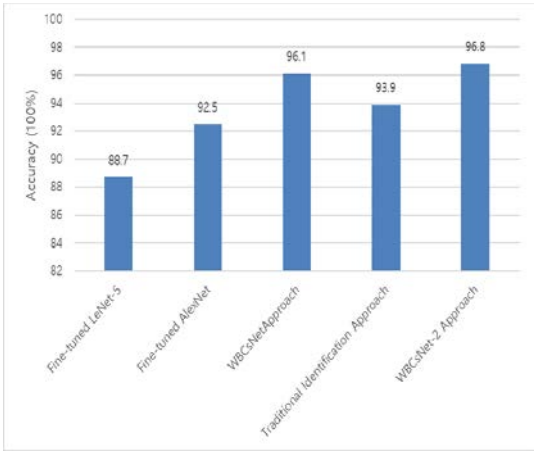

Fig. 6 The proposed WBCsNet-2 accuracy performance vs previous approaches.

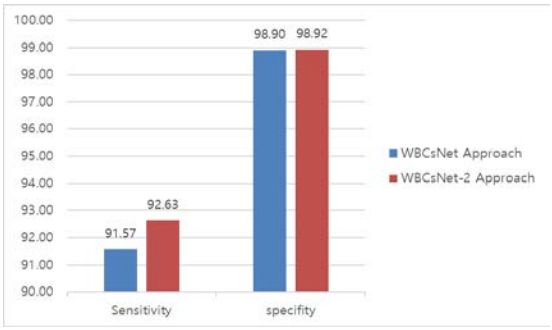

Fig. 7 The proposed WBCsNet-2 vs. WBCsNet evaluation parameters.

Table 1: Confusion matrix for WBCsNet performance.

	Rec. Neutrophil	Rec. Eosinophil	Rec. Basophil	Rec. lymphocyte	Rec. Monocyte
Neutrophil	1401	10	0	0	1
Eosinophil	13	70	0	0	0
Basophil	0	0	10	0	0
lymphocyte	0	0	0	502	15
Monocyte	10	0	0	13	119

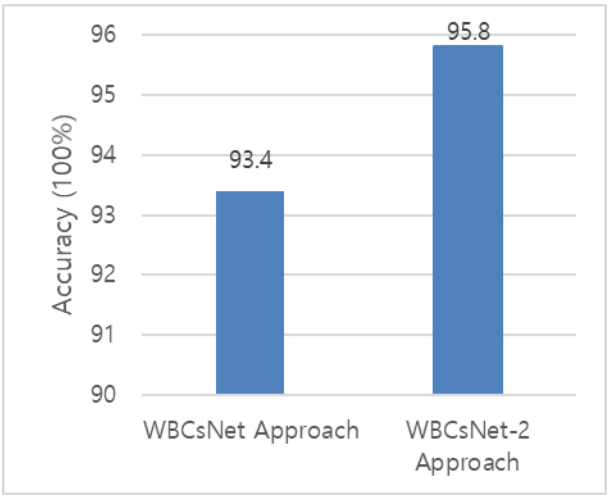

Fig. 8 The proposed WBCsNet-2 vs. WBCsNet based on transfer learning.

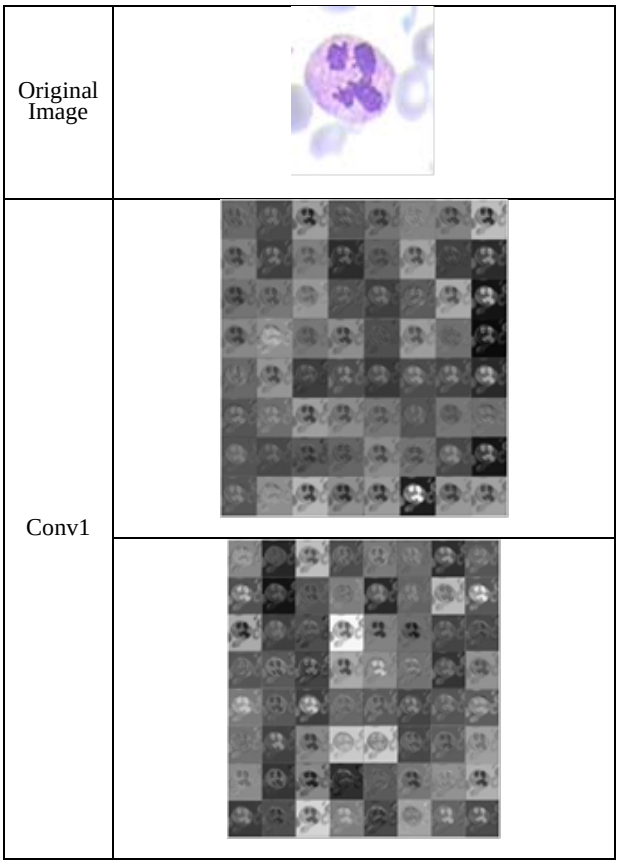

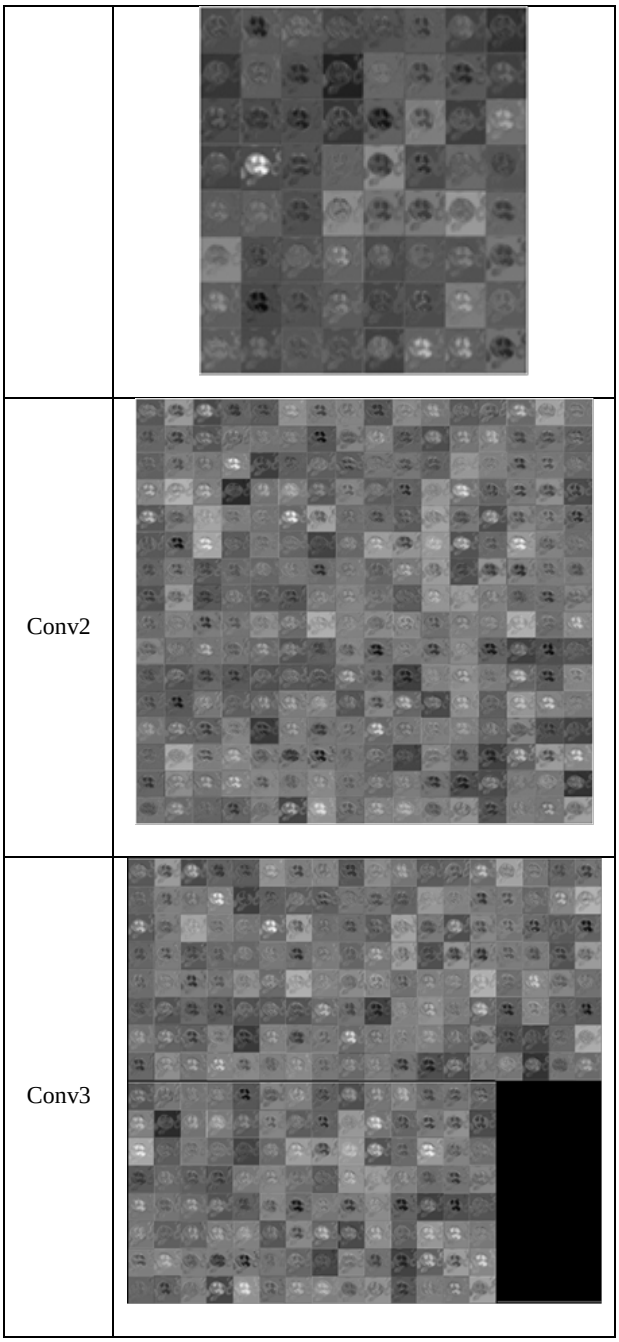

Fig. 9 CNN features visualization through WBCsNet-2 network.

5. Conclusion

In this paper, a novel WBCsNet-2 network architecture has been proposed. WBCsNet-2 modifications based on adding batch normalization and dropout layers, and residual block increased the proposed WBCsNet-2 performance. It achieved 96.8% accuracy and 92.63%

sensitivity. The cells which have large no. inside dataset, its recognition has been improved. This suggests increasing the performance of the proposed recognition system by increasing the lower cells numbers. This study has gone some way towards enhancing our understanding of residual block utilization that can be generalized to increase the other low-depth plain CNN. On the other hand, increasing WBCsNet-2 performance aims to increase WBCsNet-2 function as a pre-trained network. WBCsNet-2 as a pre-trained network has been employed successfully to recognize limited size WBCs dataset. It achieved 95.8% accuracy according to the transfer learning approach. The proposed WBCsNet-2 demonstrates high activation responses related to deep learned features. Our experimental results were very promising and suggest generalizing our methods for other medical application recognition problems.

Acknowledgement

The author would like to thank Deanship of Scientific Research, Majmaah University (Grant no. R-1441-14) for funding this work.

References

[1] CRUZ, Jennifer C. Dela, et al. Microscopic Image Analysis and Counting of Red Blood Cells and White Blood Cells in a Urine Sample. In: Proceedings of the 2019 9th International Conference on Biomedical Engineering and Technology. ACM, 2019. p. 113-118.

[2] TAVARES, Yuri Marchetti; NEDJAH, Nadia; DE MACEDO MOURELLE, Luiza. Using Neural Networks and Hough Transform for Leukocytes Differentiation in Blood Count Images. In: International Conference on Computational Science and Its Applications. Springer, Cham, 2019. p. 643-653.

[3] HEGDE, Roopa B., et al. Comparison of traditional image processing and deep learning approaches for classification of white blood cells in peripheral blood smear images. Biocybernetics and Biomedical Engineering, 2019, 39.2: 382-392.

[4] J. Wu, P. Zeng, Y. Zhou and C. Olivier, "A novel color image segmentation method and its application to white blood cell image analysis," in 8th international Conference on Signal Processing, Beijing, 2006.

[5] Q. Wang, L. Chang, M. Zhou, Q. Li, H. Liu and F. Guo, "A spectral and morphologic method for white blood cell classification," Optics & Laser Technology, vol. 84, pp. 144-148, 2016.

[6] G.Abedini, M. Firouzmand, and A.Razavi, "Recognition and Counting of WBCs using Wavelet Transform," International Journal of Emerging Trends & Technology in Computer Science, vol. 2, no. 5, 2013.

[7] S. H Rezatofighi and H. Soltanian-Zadeh, "Automatic recognition of five types of white blood cells in peripheral blood," Computerized Medical Imaging and Graphics, vol. 35, no. 4, pp. 333-343, 2011.

[8] J. Prinyakupt and C.Pluempitiwiriyawej, "Segmentation of white blood cells and comparison of cell morphology by linear and naïve Bayes classifiers," Biomedical engineering online, vol. 14, no. 1, p. 1:63, 2015.

[9] N. Ramesh, B. Dangott, M. E. Salama and T. Tasdizen, "Isolation and two-step classification of normal white blood cells in peripheral blood smears," Journal of pathology informatics, vol. 3, no. 1, p. 3:13.

[10] L. Putzu, Caocci and C. Di Ruberto, "Leucocyte classification for leukaemia detection using image processing techniques," Artificial intelligence in medicine, vol. 3, no. 62, pp. 179-191, 2014.

[11] S. Nazlibilek, D. Karacor, T. Ercan, M. H. Sazlı, O. Kalender and Y. Ege, "Automatic Segmentation, Counting, Size Determination and Classification of white blood cells," Measurement, vol. 55, pp. 58-65, 2014.

[12] A. Mathur, A. S. Tripathi and M. Kuse, "Scalable system for classifcation of white blood cells from Leishman stained blood stain images," Journal of pathology informatics, vol. 4, 2013.

[13] P. Ghosh, D. Bhattacharjee and M. Nasipuri, "Blood smear analyzer for white blood cell counting: A hybrid microscopic image analyzing technique," Applied Soft Computing, vol. 46, pp. 629-638, 2016.

[14] M. C. SU, C. Y. CHENG and P. C. WANG, "A neural-network-based approach to white blood cell classification," The Scientific World Journal 2014, pp. 1-9, 2014.

[15] HEGDE, Roopa B., et al. Feature extraction using traditional image processing and convolutional neural network methods to classify white blood cells: a study. Australasian physical & engineering sciences in medicine, 2019, 42.2: 627-638.

[16] SHARMA, Mayank; BHAVE, Aishwarya; JANGHEL, Rekh Ram. White Blood Cell Classification Using Convolutional Neural Network. In: Soft Computing and Signal Processing. Springer, Singapore, 2019. p. 135-143.

[17] RAHMAN, Aimon, et al. Improving Malaria Parasite Detection from Red Blood Cell using Deep Convolutional Neural Networks. arXiv preprint arXiv:1907.10418, 2019.

[18] RAJARAMAN, Sivaramakrishnan; JAEGER, Stefan; ANTANI, Sameer K. Performance evaluation of deep neural ensembles toward malaria parasite detection in thin-blood smear images. PeerJ, 2019, 7: e6977.

[19] Rehman, A, Abbas, N, Saba, T, Rahman, Syed Ijaz ur, Mehmood, Z, Kolivand, H. Classification of acute lymphoblastic leukemia using deep learning. Microsc Res Tech. 2018; 81: 1310– 1317. https://doi.org/10.1002/jemt.23139

[20] ZHAO, Jianwei, et al. Automatic detection and classification of leukocytes using convolutional neural networks. Medical & biological engineering & computing, 2017, 55.8: 1287-1301.

[21] WANG, Qiwei, et al. Deep learning approach to peripheral leukocyte recognition. PloS one, 2019, 14.6: e0218808.

[22] Y. LeCun, L. Bottou, Y. Bengio, and P. Haffner, "Gradient-based learning applied to document recognition," Procedding of IEEE, vol. 86, no. 18, p. 2278–2324, 1998.

[23] Alex Krizhevsky, Ilya Sutskever, and Geoffrey E. Hinton. 2017. ImageNet classification with deep convolutional neural networks. Commun. ACM 60, 6 (May 2017), 84-90. DOI: https://doi.org/10.1145/3065386.

[24] SIMONYAN, Karen; ZISSERMAN, Andrew. Very deep convolutional networks for large-scale image recognition. arXiv preprint arXiv:1409.1556, 2014.
[25] SZEGEDY, Christian, et al. Rethinking the inception architecture for computer vision. In: Proceedings of the IEEE conference on computer vision and pattern recognition. 2016. p. 2818-2826.
[26] HE, Kaiming, et al. Deep residual learning for image recognition. In: Proceedings of the IEEE conference on computer vision and pattern recognition. 2016. p. 770-778.
[27] F. Hu, G. S. Xia, J. Hu and L. Zhang, "Transferring Deep Convolutional Neural Networks for the Scene Classification of High-Resolution Remote Sensing Imagery," remote sensing, vol. 7, no. 11, pp. 14680-14707, 2015.
[28] C. Spampinato, S. Palazzoe, D. Giordanoe, M. Aldinuccie and R. Leonardie, "Deep learning for automated skeletal bone age assessment in X-ray images," Medical Image Analysis, vol. 36, p. 41–51, 2 2017.
[29] X. Gao, W. Li , M. Loomes and L. Wang, "A fused deep learning architecture for viewpoint classification of echocardiography," Information Fusion, vol. 36, pp. 103-113, 2016.
[30] Q. Zhang, Y. Xiao, W. Dai, J. Suo, C. Wang, J. Shi and H. Zheng, "Deep learning based classification of breast tumors with shear-wave elastography," Ultrasonics, vol. 72, pp. 150-157, 2016.
[31] H. K. v.d. Burgha, R.Schmidta, H. J. Westenenga, M. A. de Reusb, L. H. v. d. Berga and M. P. Heuvel, "Deep learning predictions of survival based on MRI in amyotrophic lateral sclerosis," NeuroImage: Clinical, vol. 13, pp. 361-369, 2017.
[32] N. Liu, M.Zhang, H.Li , Z.Sun and T. Tan, "DeepIris: Learning pairwise filter bank for heterogeneous iris verification," Pattern Recognition Letters, vol. 82, pp. 154-161, 2016.
[33] S.Pang , Z.Yu and M. A. Orgun, "A Novel End-to-End Classifier Using Domain Transferred Deep Convolutional Neural Networks for Biomedical Images," Computer Methods and Programs in Biomedicine, vol. 140, pp. 283–293, 2017.
[34] X. W. Gao, R. Hui and Z. Tian, "Classification of CT brain images based on deep learning networks," Computer Methods and Programs in Biomedicine , vol. 138, pp. 49-56, 2017.
[35] T. Kooi, G. Litjens, B. V. Ginneken, A G. Mérida, C. I. Sánchez, R. Mann, A. Heeten and N. Karssemeijer , "Large scale deep learning for computer aided detection of mammographic lesions," Medical Image Analysis, vol. 35, pp. 303-312, 2017.
[36] C.Szegedy, W.Liu and Y. Jia, "Going Deeper with Convolutions," arXiv [cs.CV], 2014.
[37] D. J. Hemanth, J. Anitha, A. Naaji, O. Geman, D. E. Popescu and L. Hoang Son, "A Modified Deep Convolutional Neural Network for Abnormal Brain Image Classification," in IEEE Access, vol. 7, pp. 4275-4283, 2019.
[38] A. S. Razavian, H. Azizpour, J.Sullivan and S. Carlsson , "Cnn features off-the-shelf: An astounding baseline for recognition," in Proceedings of the 2014 IEEE Conference on Computer Vision and Pattern Recognition Work-shops CVPRW, 2014.
[39] S. Jialin Pan and Q.Yang, "A Survey on Transfer Learning," IEEE Transactions on Knowledge and Data Engineering, vol. 22, no. 10, 2010.
[40] SHAHIN, A. I., et al. White blood cells identification system based on convolutional deep neural learning networks. Computer methods and programs in biomedicine, 2017.
[41] SHAHIN, A. I., et al. A novel enhancement technique for pathological microscopic image using neutrosophic similarity score scaling. Optik, 2018, 161: 84-97.
[42] PANSOMBUT, Tatdow, et al. Convolutional Neural Networks for Recognition of Lymphoblast Cell Images. Computational Intelligence and Neuroscience, 2019, 2
[43] HABIBZADEH, Mehdi; KRZYŻAK, Adam; FEVENS, Thomas. White blood cell differential counts using convolutional neural networks for low resolution images. In: International Conference on Artificial Intelligence and Soft Computing. Springer, Berlin, Heidelberg, 2013. p. 263-274.
[44] RAZZAK, Muhammad Imran; NAZ, Saeeda. Microscopic blood smear segmentation and classification using deep contour aware CNN and extreme machine learning. In: 2017 IEEE Conference on Computer Vision and Pattern Recognition Workshops (CVPRW). IEEE, 2017. p. 801-807.
[45] LECUN, Yann; BENGIO, Yoshua; HINTON, Geoffrey. Deep learning. nature, 2015, 521.7553: 436.
[46] GU, Jiuxiang, et al. Recent advances in convolutional neural networks. Pattern Recognition, 2018, 77: 354-377.
[47] BISHOP, Christopher M. Pattern recognition and machine learning. springer, 2006.